Tensile Drawing Behaviour of Polyethylene Terephthalate

S. D. LONG and I. M. WARD*

IRC in Polymer Science and Technology, University of Leeds, Leeds LS2 9JT, UK

SYNOPSIS

A wide range of polyethylene terephthalate fibres was prepared by melt spinning to different degrees of molecular orientation. The tensile drawing behaviour of these fibers was then studied, either by drawing over a heated cylinder at 85°C or by drawing over both a heated cylinder and a plate at 180°C. The mechanical properties and structure of the subsequent drawn fibres are discussed in terms of the network draw ratio, determined by matching true stress–strain curves for the drawn and initial melt spun fibres. It is shown that this procedure provides valuable insight into subtle differences in properties and structure that can arise from differences in processing routes.

INTRODUCTION

The drawing behaviour of polyethylene terephthalate has been the subject of many investigations. Recent studies primarily concerned with fibres spun at high wind-up speeds include those of Brody[1,2] and Heuvel and Huisman.[3] One issue that has been of some interest in both these later studies, as well as in earlier work,[4] has been the continuity of a molecular network throughout the spinning and drawing processes. The existence of a molecular network was revealed by stress-optical measurements on spun and drawn yarns[5,6] and has been confirmed by examination of the strain-hardening behaviour of drawn yarns.[1]

The present article describes a comprehensive study of pin drawing and pin and plate drawing of a series of spun yarns, prepared over a wide range of wind-up speeds. This produces yarns of different orientation and morphology, prior to drawing. The differences between pin drawing and pin and plate drawing are examined. Mechanical measurements of modulus, breaking stress, and breaking extensibility are combined with the determination of crystallinity, amorphous orientation, and network draw ratio to provide insight into the mechanisms of deformation that occur in the drawing processes and how these affect final yarn properties.

* To whom correspondence should be addressed.

Journal of Applied Polymer Science, Vol. 42, 1911–1920 (1991)
 CCC 0021-8995/91/071911-10$04.00

EXPERIMENTAL

Preparation of the Precursor Spun Yarns

Three groups of precursor spun yarns were produced by melt spinning under different conditions at Hoechst Celanese in Charlotte, North Carolina, U.S.A. Details of the preparation procedures are given in Table I. In the first group (yarns A–H), all feed stocks were spun at a spinning temperature (T_s) of 292°C and the wind-up speed (WUS) was varied between 0.5–4.6 km/min. The second group (yarns 1–4) were spun at T_s = 300°C and WUS in the range 3.5–5.5 km/min. The third group (yarns 5–10) consisted of yarns spun at T_s = 290°C at WUS of 3.0, 4.0, and 5.0 km/min with two yarns at each speed, differing only in filament diameter.

Drawing Procedures

A first set of drawn fibres was produced by drawing over a heated cylinder (the pin) at 85°C to a series of draw ratios, called pin-drawn yarns.

A second set (pin- and plate-drawn yarn) was produced by drawing over a pin at 85°C, followed by a plate at 180°C.

Tensile Testing

Fibre samples of 10 cm gauge length were extended at an initial strain rate of 0.5 min^{-1} on a conventional Instron tensile tester. The initial modulus was

Table I Preparation Procedures for Spun Yarns

Series	Wind-up Speed (km/min)	Intrinsic Viscosity	Spinning Temperature T_s (°C)
1 (A–H)	0.46–4.57	0.62	292
2 (1–4)	3.50–5.50	0.64	300
3 (5–10)	3.00–5.00	0.64	290

obtained from the gradient of the linear region of the load-extension chart. To obtain reliable moduli, a large magnification was applied to the extension axis.

Birefringence

Birefringence measurements were made on a Carl Zeiss Polmi A microscope equipped with an Ehringhaus compensator.

Density

Specimen densities were obtained from an aqueous potassium iodide density column.

Measurement of Network Draw Ratio

The network draw ratio has been determined from a combination of two types of measurement. First, the measurement of shrinkage and shrinkage force showed that precursor A, the yarn of lowest wind-up speed, has a very low network draw ratio of 1.07. Second, the network draw ratio of all other precursor yarns was determined following a slight modification of the method proposed by Brody.[1] The load-extension curves for the precursor yarns were obtained by drawing on an Instron tensile testing machine at room temperature and converted to true stress-natural (logarithmic) strain on the assumption of constant volume. The higher wind-up speed precursors were then superimposed on the lowest wind-up speed yarn A to produce a strain axis shift. The network draw ratio λ_{ms} of a precursor yarn is then given as

$$\lambda_{ms} = \lambda_A \lambda_x, \tag{1}$$

where λ_A is the network draw ratio of precursor A and λ_x is the strain axis shift draw ratio for yarn x. The total network draw ratio for a drawn yarn is then given as

$$\lambda_{\text{net}} = \lambda_{ms} \lambda_{hd}, \tag{2}$$

where λ_{hd} is the imposed draw ratio.

Determination of Crystallinity and Amorphous Orientation

The crystalline volume fraction V_c is calculated from the sample density ρ on the basis of the formula

$$V_c = \frac{(\rho - \rho_a)}{\rho_c - \rho_a}, \tag{3}$$

where ρ_c and ρ_a are the densities of the crystalline and amorphous phases, respectively.

Recent work by Fakirov et al.[7] shows that ρ_c is dependent on the crystallisation conditions. We have followed their findings and assumed that the yarn drawn over a pin at 85°C will be equivalent to yarn crystallised at low temperatures where a value of $\rho_c = 1484$ kg m^{-3} is appropriate. Using a plate at 180°C is considered equivalent to annealing under strain, and a higher value of $\rho_c = 1515$ kg m^{-3} has therefore been assumed.

Studies of high wind-up speed yarns by Heuval and Huisman[3] showed a variation in ρ_c from 1488 kg m^{-3} at 4.7 km/min to 1501 kg m^{-3} at 6.0 km/min. We have used their values of ρ_c for the high wind-up speed yarns in the present investigation and a value of 1484 kg m^{-3} for the lower wind-up speed yarns.

The amorphous density ρ_a was calculated using the formula of Heuval and Huisman[3]:

$$\rho_a = 1336 + 9.4 f_a, \tag{4}$$

where f_a is the amorphous orientation. This was calculated by an iterative procedure using the eqs. (3) and (4) with the relationship

$$f_a = \frac{\Delta n - V_c f_c \Delta n_c^0}{(1 - V_c)\Delta n_a^0}, \tag{5}$$

where $\Delta n_c^0 = 0.22$, $\Delta n_a^0 = 0.24$, and Δn is the specimen birefringence.

In general, the values of ρ_a, V_c, and f_a became constant after three iterations, but a fourth iteration was performed in all instances to ensure consistency. From the previous work of Heuval and Huisman, f_c for the precursor yarns was assumed to be 0.97. Following Padibjo and Ward,[8] the value of f_c for pin-only yarn was taken to be 0.90, and for pin and plate drawing a value of 0.935 was assumed, which is between that of the spun yarn and the pin-only yarns.

Theoretical Estimate of Extensional Modulus

It will prove instructive to compare the measured extensional moduli with those predicted from simple

modelling. Following Samuels,[9] the extensional modulus E_0 is given by

$$\frac{3}{2E_0} = \frac{V_c(1-f_c)}{E_{90}^c} + \frac{(1-V_c)(1-f_a)}{E_{90}^a},$$

where E_{90}^c and E_{90}^a are the intrinsic moduli of the crystalline and amorphous regions, respectively, in the direction normal to the fibre axis. Knowing that E_0 = 2 GPa for unoriented amorphous PET, E_{90}^a was calculated using the above expression. In this case, $V_c = 0$, $f_a = 0$, and $f_c = 0$:

$$E_{90}^a = \frac{2E_0}{3}.$$

E_{90}^c was assumed to be similar to that quoted for polybutylene terephthalate.[10]

Infrared Spectroscopy

The spun and drawn yarns were examined by polarised infrared spectroscopy following the procedures devised by Yazdanian et al.[11] A filament winding operation was used to produce a parallel grid of fibres on a KBr plate. The infrared spectra of the fibre grids were recorded with a Perkin–Elmer 580B ratio recording spectrometer. The analysis of the spectra was undertaken with computer fitting procedures described in detail in previous publications.[11,12]

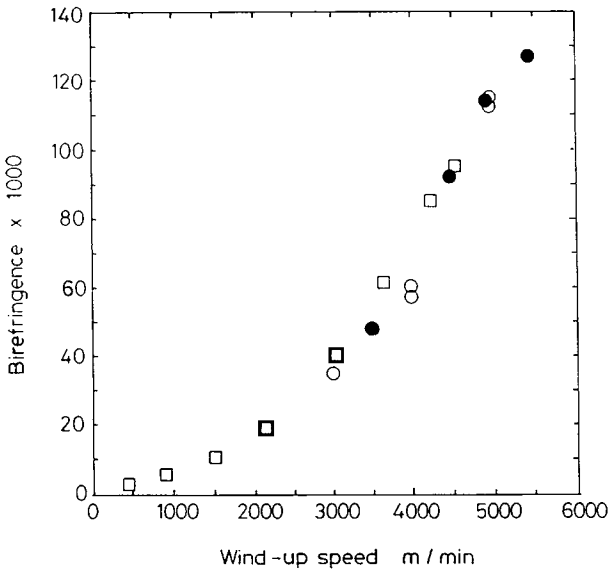

Figure 1 Birefringence vs. wind-up speed for spun yarns. Spinning temperature: □, T_s 292°C; ●, T_s 300°C; ○, T_s 290°C.

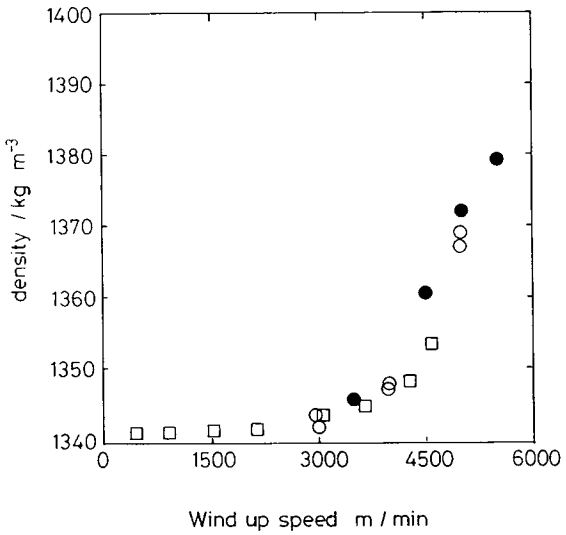

Figure 2 Density vs. wind-up speed for spun yarns. □, T_s 292°C; ●, T_s 300°C, ○, T_s 290°C.

RESULTS

Spun Yarns

In Figure 1, the birefringence is seen to rise smoothly with wind-up speed, and there are only very small effects due to spinning temperature and filament diameter. On the other hand, Figure 2 shows the density to rise sharply at about 3.5 km/min where crystallisation occurs, which was confirmed by wide angle X-ray diffraction measurements. Yarns spun at the highest T_s show the greatest rise in density.

The true stress–strain curves for the series of yarns spun at 292°C are shown in Figure 3. In Figure

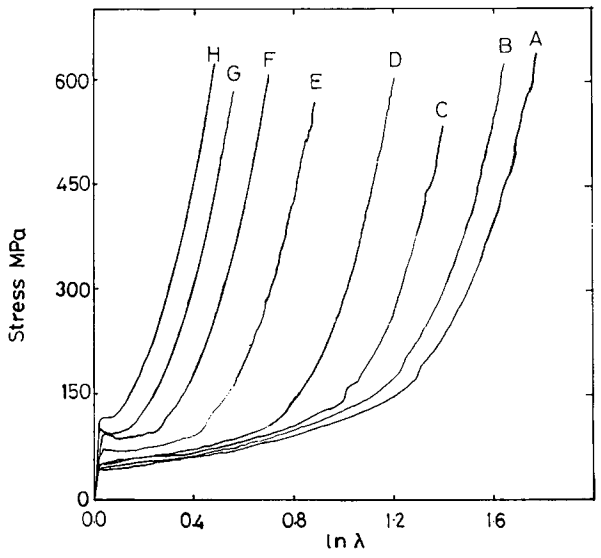

Figure 3 True stress–strain curves for spun yarns.

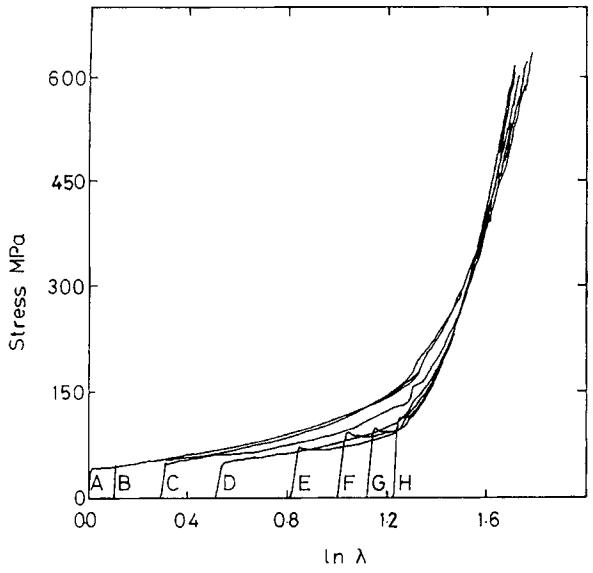

Figure 4 Matching of true stress–strain curves for spun yarns.

4, these curves have been matched against the lowest orientation precursor yarn by a horizontal shift to give a value of the network draw ratio. It can be seen that the match is a good first approximation, but there are differences in that the higher wind-up speed yarns that have crystallised show a higher rate of strain hardening, as might be expected.

Drawn Yarns

Figures 5 and 6 show the birefringence and initial modulus of the pin-drawn yarns as a function of actual drawn ratio (a) and network draw ratio (b). It can be seen that the results are very well unified by the use of the network draw ratio, and that this brings together both the spun and drawn yarns. The concept of a network that maintains its existence throughout the spinning and subsequent drawing process is further substantiated by the results for the breaking extensibility of both the precursor and pin-drawn yarns shown in Figure 7. It appears that there is a limiting total extensibility of the network formed during spinning, and break occurs at a stress of about 600 MPa, as can be seen for the precursor yarns by inspection of Figure 3.

The results for pin- and plate-drawn yarns are at first sight similar to those for the pin-drawn yarns in that the variations of birefringence and modulus with processing can be unified to a good approximation by the use of the network draw ratio (Figs. 8 and 9), although there is a good deal more scatter on the plots at the higher values of network draw ratio. A more important distinction between pin drawing and pin and plate drawing is, however, illustrated in Figure 10, where comparative room temperature stress–strain curves are shown for drawn yarns prepared from one of the highest wind-up speed precursors. It can be seen that the pin-only drawn yarns show a yield point and an ultimate breaking stress of about 600 MPa, which is similar to that of the precursors (Fig. 3). The pin- and plate-drawn yarns, on the other hand, show no yield drop and higher breaking stresses than the precursors, rising to 1 GPa at the highest draw ratio. This comparison of the stress–strain curves indicates that the pin and plate drawing process produces oriented material with much enhanced strain hardening characteristics. A curve such as that shown in Figure 10(d) suggests that there is a much more homogeneous distribution of stress in the molecular struc-

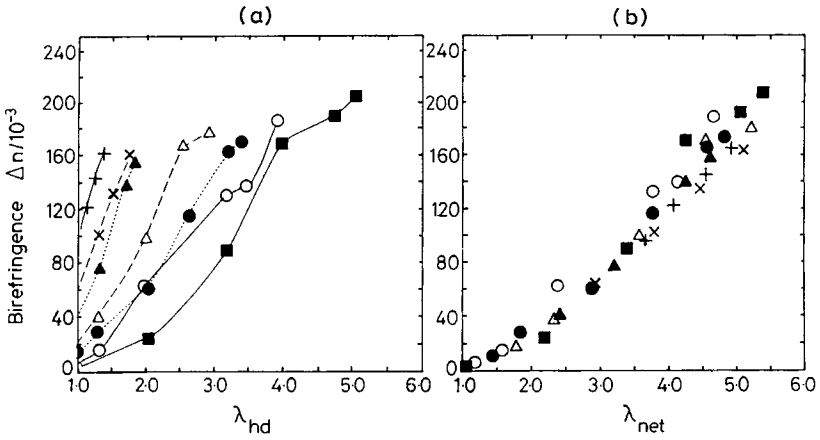

Figure 5 Birefringence vs. actual draw ratio λ_{hd} (a) and network draw ratio λ_{net} (b) for pin-drawn yarns and their precursors. ■, A; ○, B; ●, C; △, D; ▲, E; ×, F; +, H.

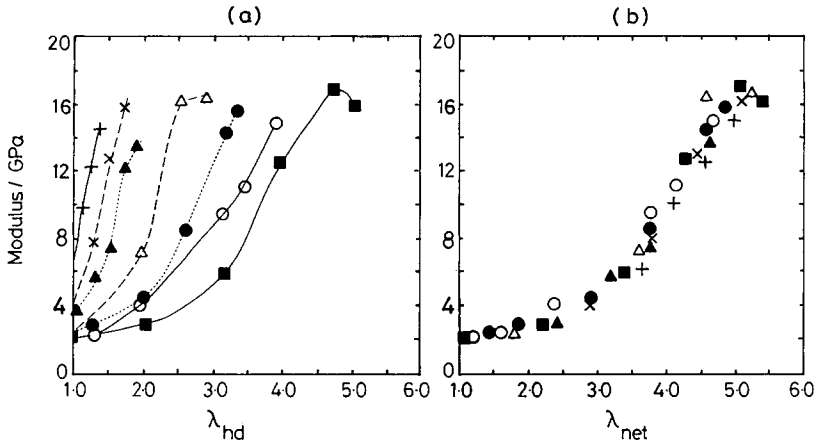

Figure 6 Initial modulus vs. actual draw ratio λ_{hd} (a) and network draw ratio λ_{net} (b) for pin-drawn yarns and their precursors (symbols as in Fig. 5).

ture than in the case of the pin-drawn yarns, where there is a yield and fracture. These results suggest that the network structure formed during the spinning thread-line has been modified by the pin and plate drawing process. This conclusion is substantiated by matching the stress–strain curves of precursor and drawn yarns, shown in Figures 11(a) and (b). It can clearly be seen that pin and plate drawing increases the breaking extensibility. The network structure is modified during drawing so that greater overall extension can be obtained before failure.

Comparison of Figures 8 and 12 shows the variation of f_a with λ_{net} to be very similar to that of birefringence with λ_{net}. It must be concluded that the calculation described earlier is unable to give values of f_a that are independent of the birefringence, even for the relatively high crystallinity pin and plate yarns.

DISCUSSION

Spinning Process

Differences in the stress–strain curves for the spun yarns precursors are small, and can be attributed to crystallisation in the threadline above the critical speed of about 3.5 km/min rather than major mod-

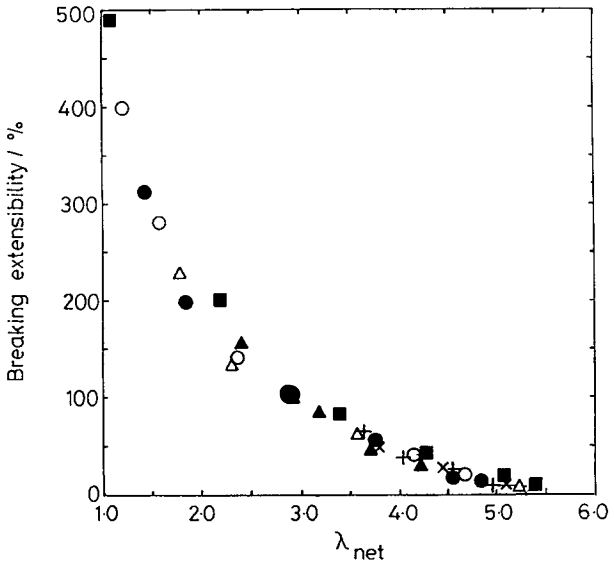

Figure 7 Breaking extensibility vs. network draw ratio λ_{net} for pin-drawn yarns and their precursors (symbols as in Fig. 5).

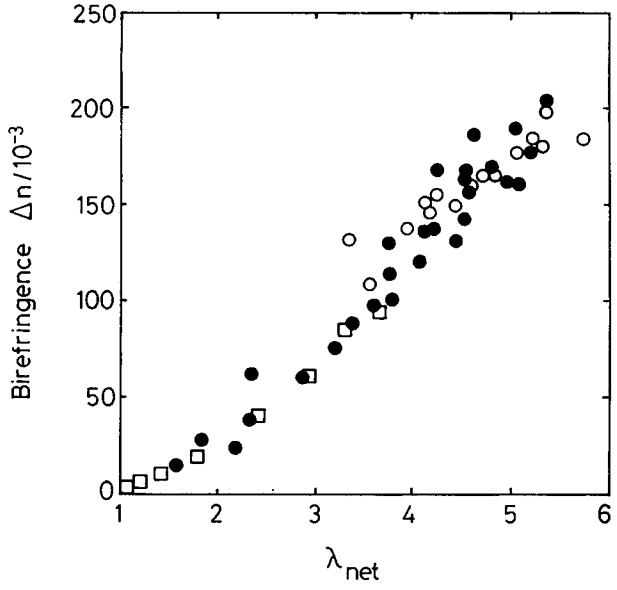

Figure 8 Birefringence vs. network draw ratio λ_{net} for spun precursors □, pin-only yarns ●, and pin and plate yarns ○.

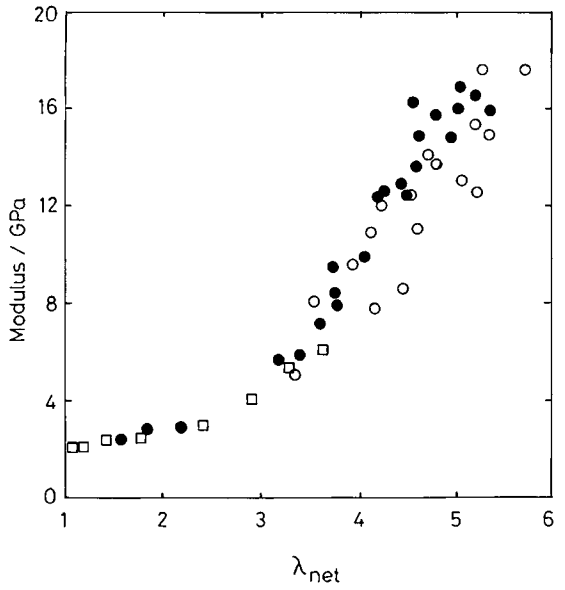

Figure 9 Initial modulus vs. network draw ratio λ_{net} for spun precursors □, pin-only yarns ●, and pin and plate yarns ○.

ifications of the molecular network with increasing wind-up speed. The total network draw ratio (including the extension to break of the drawn yarn) falls from a maximum of 6.3 for precursor yarn *A* to about 6.0 for the other precursors, suggesting that

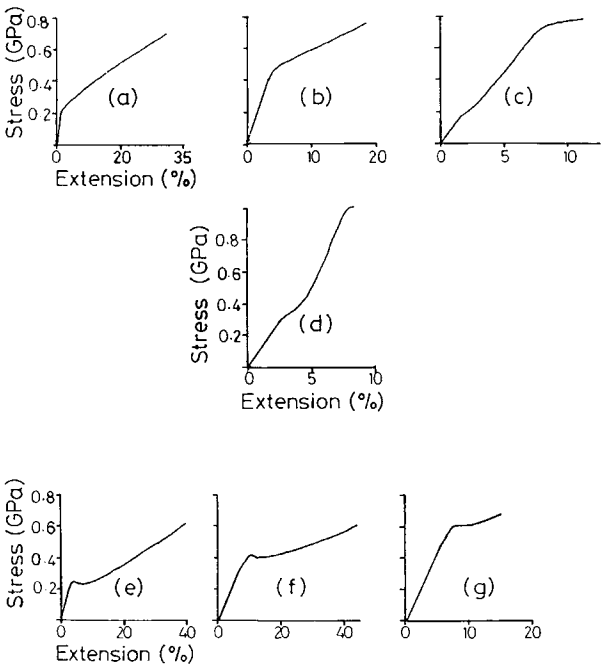

Figure 10 Room temperature stress–strain curves. (a)–(d), pin- and plate-drawn yarns; (e)–(g) pin-only drawn yarns.

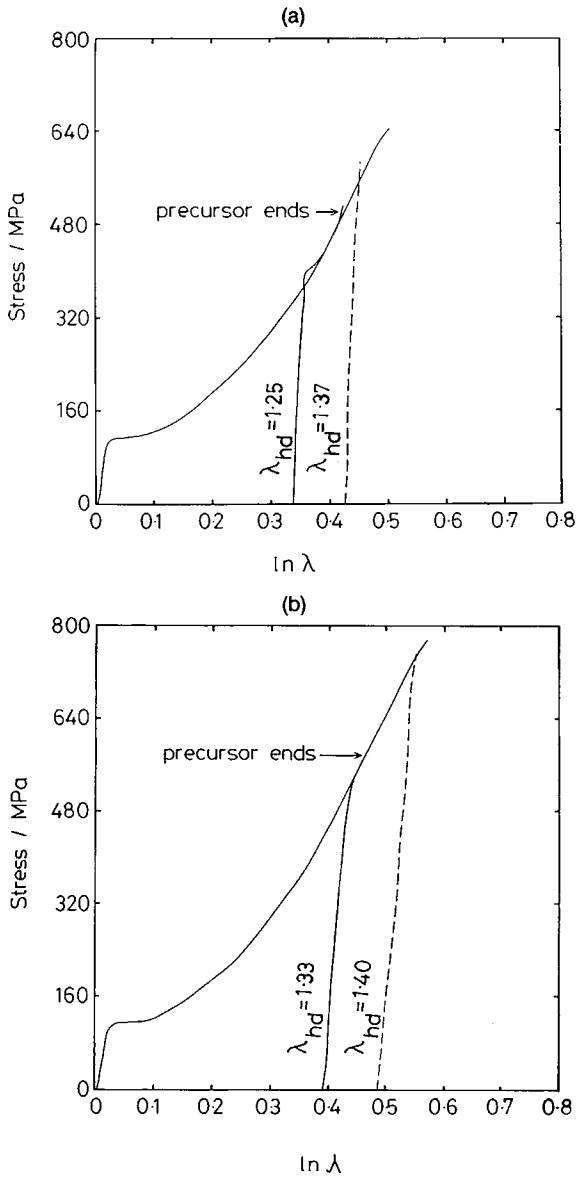

Figure 11 Matching of true stress–strain curves for (a) pin-drawn yarn and (b) pin- and plate-drawn yarn from the high wind-up speed precursor *H*.

there is a gradual change in the network with increasing wind-up speed, but this is a very small effect compared with changes that can be induced by the drawing process, as has been shown.

Pin-Drawing Process

The pin-drawing process also does not appear to greatly alter the nature of the molecular network. It is especially to be noted that pin-drawn yarns lie on the same path as the precursor spun yarns for plots of birefringence vs. network draw ratio, with

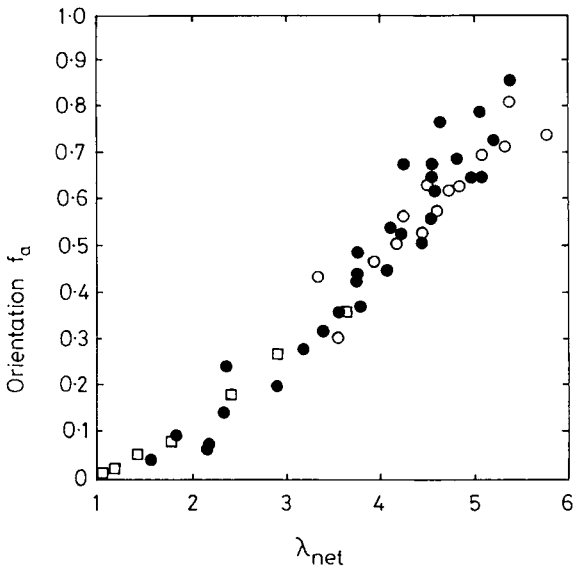

Figure 12 Amorphous orientated f_a vs. network draw ratio λ_{net}. □, as spun; ■, pin only; ○, pin and plate.

some scatter about $\lambda_{net} > 3.5$ where crystallisation occurs. It is also to be noted that the extension to break of the pin-drawn yarns is very similar to that of the precursors, further confirmation that the network is not modified significantly during pin drawing.

There is a better correlation between initial modulus and the network draw ratio λ_{net} than for that between birefringence or amorphous orientation and λ_{net}. This may indicate a "biasing" of the network with increasing wind-up speed, as suggested by Brody,[2] and it may be considered that initial modulus reflects the extension of the network better than birefringence which is affected by structural factors such as crystallinity, which do not relate directly to the load-bearing capacity. The idea is that the number of shortest chains at a given value of λ_{net} is constant for different processing results, giving a similar modulus, but the distribution of tie molecules widens with increasing wind-up speed, resulting in lower values of birefringence and amorphous orientation. This concept of network bias has also proved useful in understanding shrinkage force and free shrinkage results for these materials, reported in the accompanying paper.[13]

The stress–strain curves for the pin-drawn yarns show a clear yield point, followed by cold drawing and then homogeneous extension to failure. This behaviour is seen even for drawn yarns from the highest wind-up speed precursors. There is a loss of orientation during pin drawing that leads to a loss of molecular orientation that is only regained in the strain-hardening region where cold drawing is taking place. This leads to a final degree of orientation very comparable to that achieved by cold drawing at room temperature, which is being used to determine λ_{net}, i.e., with regard to the molecular network (but not necessarily the morphology of the drawn yarn) cold drawing and drawing over a heated pin at 85°C appear to be comparable.

In the pin-drawing process, the heated pin is positioned between the feed and draw rollers in a way that allows the yarn to be extended on the pin itself. Following orientation on the pin, the yarn is able to relax, leading to a loss of molecular orientation. This relaxation can be inferred in that the pin-only process resulted in a lower geometric draw ratio than pin and plate drawing at the same machine draw ratio. As mentioned in the following section, pin and plate drawing prevents this relaxation, which was observed during the drawing treatments. In the pin and plate case, there was little difference between the machine and geometric draw ratios. Clearly, the addition of the heated plate helps prevent the relaxation of the drawn yarn.

It should be noted that when an intermediate wind-up speed precursor (2.1 km/min) was pin drawn there was an increase in breaking stress at the highest λ_{net}, suggesting that each feedstock yarn has its own optimum drawing conditions, which should (ideally) be experimentally determined.

Pin- and Plate-Drawing Process

The pin and plate drawing of low wind-up speed yarns, where significant crystallisation does not occur in the threadline, appears to give very similar products to the pin drawing of all yarns, irrespective of wind-up speed. Some differences are detectable at the highest wind-up speeds, where the network may be slightly modified, but these are comparatively small. The most dramatic changes in the final yarn properties are obtained for the pin and plate drawing of high wind-up speed yarns where outstanding mechanical strengths can be achieved. The stress–strain curves of these drawn yarns are different in character from the pin-drawn yarns. It appears that the crystallisation of the pin- and plate-drawn yarns introduced by the addition of the heated plate prevents the loss of orientation. The clear yield point is not present, and there is a much more rapid strain-hardening.

The loss of orientation during pin drawing must be eliminated if significant further work-hardening is to take place. Following yielding, viscous flow occurs, which involves untangling and orientation of the network chains. As these chains become taut,

work-hardening is observed. This relaxation does not occur in the pin and plate process because secondary crystallisation intervenes immediately, "setting in" the orientation. Even more important, it appears that the original network has been modified so that a greater overall extensibility and hence a higher degree of molecular orientation can be achieved. It is suggested that the introduction of the heated plate allows further drawing to occur over the plate at high temperatures where some of the limiting entanglements can be drawn out to give a much enhanced network extensibility. This increased extensibility is shown very clearly by the further data on the matching of the true stress–strain curves shown in Figure 11(b).

The exceptional breaking strengths of the pin and plate yarns cannot be accounted for solely on the basis of the increased total network extensibility compared to the pin-drawn yarns. Figure 13 illustrates this point, showing separate relationships between breaking stress and λ_{net} for the two processes. The pin and plate yarns show a sharp rise in strength at the highest draw ratios.

A subsidiary experiment has been carried out that involved the unconstrained shrinkage of the pin- and plate-drawn yarns at relatively high temperatures ($\sim$ 140°C). These shrunk yarns were then cold drawn. It the network draw ratio is adjusted to account for the very low shrinkages observed, it was found that the breaking stresses fell on the upper curve in Figure 13. This interesting result confirms

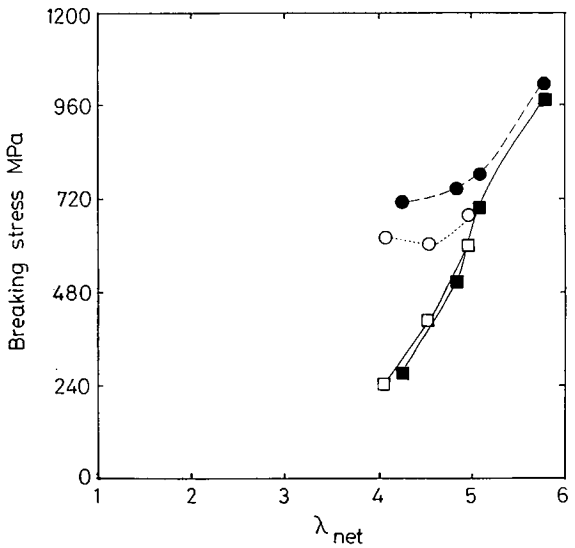

Figure 13 Comparison of ultimate breaking stress vs. network draw ratio λ_{net} for □ ○ pin-drawn and ■ ● pin- and plate-drawn yarns from the high wind-up speed precursor *H*.

Table II Comparison of λ_{net} (From Matching Stress–Strain Curves) and λ_{hd} (Measured Hot Draw Ratio)

Process	λ_{hd}	λ_{net}	$\lambda_{hd}/\lambda_{net}$
Pin only	1.25	1.40	0.89
	1.37	1.53	0.89
Pin and plate	1.33	1.48	0.90
	1.40	1.62	0.86

the dependence of the ultimate yarn properties on the drawn yarn λ_{net}.

Network Draw Ratio of Drawn Yarns

The initial strategy employed in this investigation described in the experimental section above was to use the matching of the stress–strain curves to find the effective network draw ratio for the precursor spun yarns, but to obtain a value for the further draw ratio occurring in the drawing processes from the change in dimensions of the yarn. The observation that the network might be modified by the drawing process led to the recognition that this procedure is inadequate and should be replaced by the matching of the true stress–strain curve for the drawn yarn to that of its precursor spun yarn. Table II compares values for λ_{net} obtained from the two routes and shows that λ_{hd}, determined from changes in macroscopic dimensions, is an underestimate of the true molecular network draw ratio. It is interesting to note that the ratio of the two estimates is approximately constant regardless of the process and, of coure, to recall that the molecular network is preserved at very high overall deformation in spite of clear differences in orientation and structure.

Initial Modulus

Examination of the initial modulus data (Fig. 9) shows a good approximate correlation between modulus and λ_{net}, as anticipated. The highest wind-up speed yarns drawn by the pin and plate route are unusual, as discussed above, because the network is changed by the drawing process. For the other cases, where the network is not so modified, it can be seen that the pin and plate process gives higher moduli for a given λ_{net} at low values of λ_{net} and vice versa for pin-only yarns. This results from the complex relationship between modulus and both orientation and crystallinity. As shown in Figure 9, the reduction in modulus due to the addition of the heated plate is more distinct than the drop in amorphous ori-

entation or birefringence. It can be proposed that the increased crystallinity of the pin and plate yarns leads to secondary crystallisation, which nucleates on the highly oriented structure. This can give rise to an increase in birefringence but no increase in modulus because the new highly oriented material is not load-bearing. These ideas have been previously discussed by Brody[2] and by Yazdanian et al.[10]

Figure 14 shows an attempt to fit the results to the Samuels' model. Although there is a good correlation between the theoretical and experimental values, the theory is clearly not adequate. Moreover, even the correlation is poor for pin and plate yarns where this complication of non-load-bearing oriented material is not accommodated by the model. Although Figure 14 shows the deviation of pin and plate results from those of the pin-drawn and precursor yarns, the presentation of the data in compliance form effectively reduces the large differences in modulus between the two drawing treatments, which is brought out very clearly in Figure 9.

Infrared Spectroscopy

The infrared results on these materials are described in detail elsewhere.[14] The key results with regard to the present investigation relate to the following features.

First, it was interesting to observe the presence of the 989 cm^{-1} fold band in both a highly crystalline

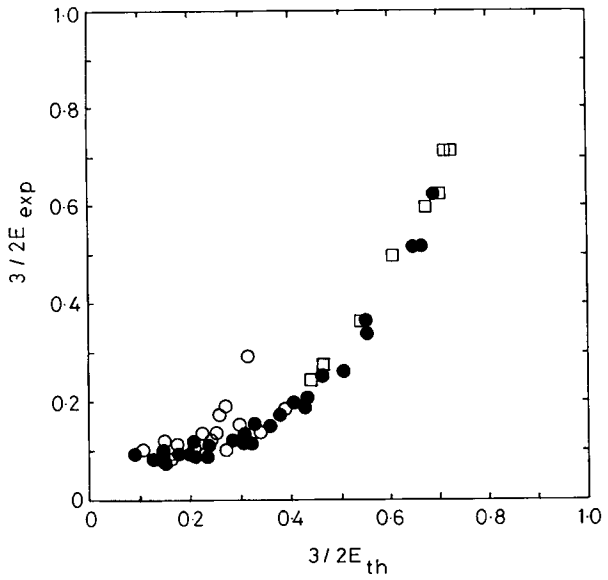

Figure 14 Attempt to fit data to Samuel's model. □, spun precursor yarns; ●, pin-only yarns; ○, pin and plate yarns; E_{exp} = measured initial modulus; E_{th} = predicted modulus.

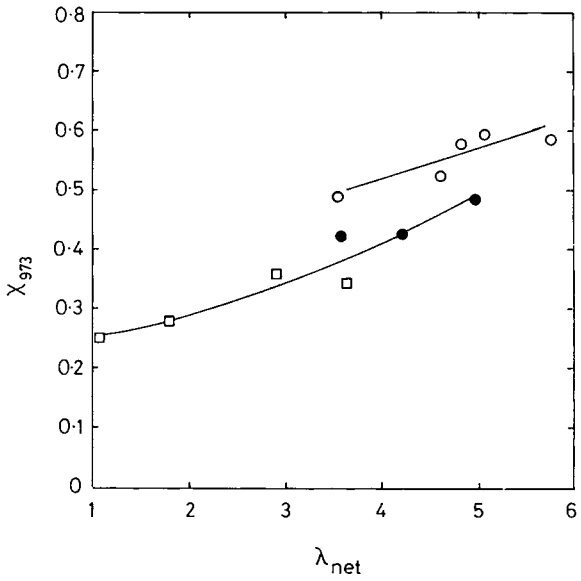

Figure 15 Trans fraction (973 cm^{-1} band) χ_{973} vs. network draw ratio λ_{net}. □, as spun; ●, pin only; ○, pin and plate.

annealed yarn and also in the pin- and plate-drawn yarns. The intensity of this 989 cm^{-1} band reduced at high values of λ_{net}, suggesting that the secondary crystallisation is chain-folded in nature and that chain-folding is lower at high network strains, leading to a reduction in network bias and an increase in breaking stress.

Second, Figure 15 shows a greater concentration of the fraction of material associated with the 973 cm^{-1} trans band to exist in the pin and plate material compared to the as-spun and pin-drawn yarns. Figure 16 shows that there is a good correlation between the breaking stress and the concentration of conformers associated with the 973 cm^{-1} trans band, except perhaps for the most highly drawn pin and plate yarns. This result is consistent with the conclusions of Yazdanian et al.,[11] where the 973 cm^{-1} trans conformation was considered to be load-bearing, and appeared to be the major constituent of the "backbone" molecules that carry the load and determine the modulus.

CONCLUSIONS

It has been shown that the use of a network draw ratio provides a valuable basis on which to compare the properties and structure of drawn polyethylene terephthalate fibres. In this way, it is possible to combine the deformations introduced at the spin-

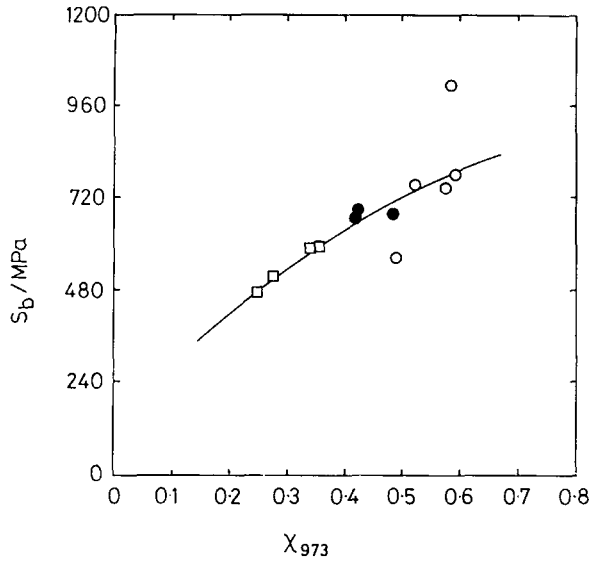

Figure 16 Breaking stress S_b vs. trans fraction χ_{973}. □, as spun; ●, pin only; ○, pin and plate.

ning and drawing stages to gain an understanding of the differences in properties that arise from different processing routes. It is of particular interest that in this respect pin and plate drawing gives rise to better ultimate properties than those obtained by drawing over a pin only. The improved properties are attributed partly to the reduction in network shrinkage occurring during drawing, and partly (and more tentatively) to a possible modification of the network during pin and plate drawing.

We are greatly indebted to our colleagues at Hoechst Celanese and Leeds University for their advice and support, especially Dr. W. Bessey at Charlotte and Dr. H. Brody and Mr. D. L. M. Cansfield at Leeds. The research project was funded by Hoechst Celanese Fibers Division, Charlotte, NC, U.S.A.

REFERENCES

1. H. Brody, *J. Macromol. Sci. Phys.* **B22**(1), 19 (1983).
2. H. Brody, *J. Macromol. Sci. Phys.* **B22**(3), 407 (1983).
3. H. M. Heuval and R. Huisman, *J. Appl. Polym. Sci.* **22,** 2229 (1978).
4. S. W. Allison, P. R. Pinnock, and I. M. Ward, *Polymer* **7,** 66 (1966).
5. P. R. Pinnock and I. M. Ward, *Trans. Faraday Soc.* **62,** 1308 (1966).
6. F. Reitsch, R. A. Duckett, and I. M. Ward, *Polymer* **20,** 1133 (1979).
7. S. Fakirov, E. W. Fischer, and G. F. Schmidt, *Makromol. Chem.* **176,** 2459 (1975).
8. S. R. Padibjo and I. M. Ward, *Polymer* **24,** 1103 (1983).
9. R. J. Samuels, *Structured Polymer Properties,* Wiley-Interscience, New York (1974).
10. I. M. Ward, in *Development in Oriented Polymers—1,* Chap. 5, I. M. Ward, Ed., Applied Science Publishers, London (1982).
11. M. Yazdanian, I. M. Ward, and H. Brody, *Polymer* **26,** 1779 (1985).
12. I. J. Hutchinson, I. M. Ward, H. A. Willis, and V. Zichy, *Polymer* **21,** 55 (1980).
13. S. D. Long and I. M. Waid, *J. Appl. Polym. Sci.,* 42, 1921 (1990).
14. S. D. Long, Ph.D. thesis, Leeds University (1989).

Received March 12, 1990
Accepted July 9, 1990